Fluorescent Probes

Subjects: Chemistry, Medicinal

Contributor: Zixin Liu , Shanyan Mo , Zhenming Hao , Liming Hu

Peroxynitrite ($ONOO^-$) is a crucial reactive oxygen species that plays a vital role in cellular signal transduction and homeostatic regulation. Determining and visualizing peroxynitrite accurately in biological systems is important for understanding its roles in physiological and pathological activity.

peroxynitrite fluorescent probes intracellular imaging

1. Introduction

Peroxynitrite ($ONOO^-$) is a kind of reactive oxygen species (ROS) generated by the rapid reaction of nitric oxide (NO) and a superoxide anion free radical ($O_2\cdot^-$) in the absence of enzyme catalysis, which has strong oxidation, nucleophilic, and nitration properties [1]. It occupies crucial roles in the transformations of other major reactive species. (Scheme 1) Its pKa value is 6.8 [2], and the half-life is approximately 1 s [3][4] at pH 7.4. $ONOO^-$ can react with a variety of bioactive substances (such as protein, nucleic acid, lipid, etc.) with very high reactivity. In addition to its oxidation, nucleophilic, and nitration properties, $ONOO^-$ can also be converted into higher activity secondary free radicals, including hydroxyl radicals (·OH), nitro radicals ($\cdot NO_2$), and carbonate radicals ($CO_3\cdot^-$), which further react with biomolecules and ultimately lead to cell death.

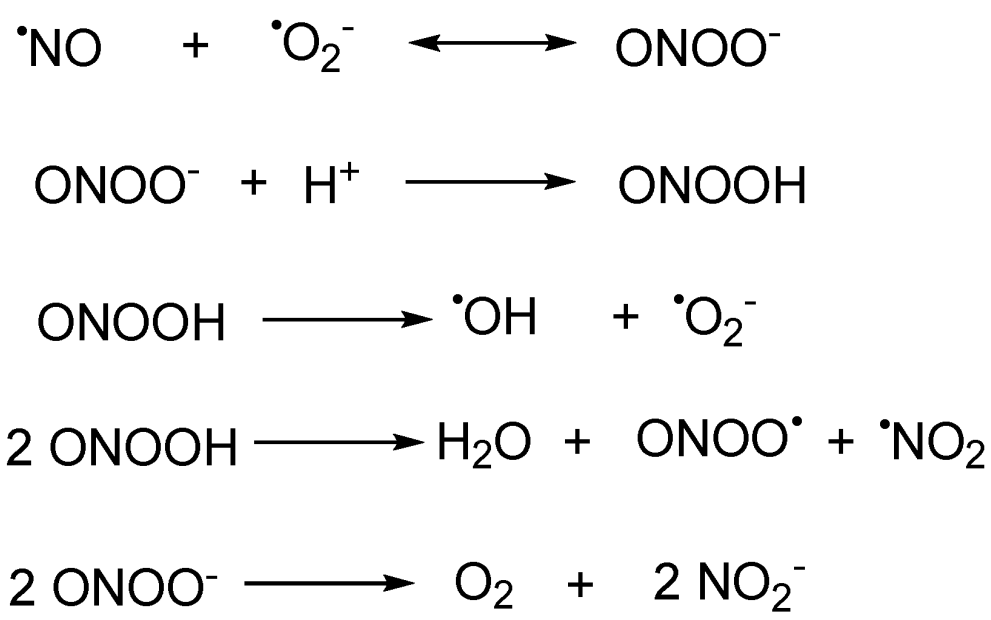

Scheme 1. The biogenesis of peroxynitrite and its transformations with other major reactive species.

Based on these properties, peroxynitrite exhibits two effects with different directions. In the living system, when the $ONOO^-$ remains at a level which is under normal physiological conditions, it serves as an indispensable physiological activator and signaling molecule. However, when the concentration of $ONOO^-$ elevates, the excess $ONOO^-$ will turn the redox state of the cell to a pro-oxidant state [5][6]. Eventually, serious inflammation and disease will be induced, for example, rheumatism, hepatic disease, neurodegenerative disease, cancer, and so on [7][8][9][10]. Therefore, it would be of great significance to develop a method which could accurately detect $ONOO^-$ and explore the physiological role of $ONOO^-$ in living systems.

In comparison to other $ONOO^-$ detection methods (positron emission computed tomography (PET), computed tomography (CT), magnetic resonance imaging (MRI), and genetically encoded indicators) [11], spectroscopic detections, especially fluorescent probes, possess advantages such as excellent temporal and spatial resolution, simple operation, high sensitivity and selectivity, and non-destructive and in situ real-time visualization of biological samples [12][13][14][15].

2. Fluorescent Probes

2.1. Xanthene as Fluorophore Core

Xanthene dyes can be categorized as fluorescein, rhodol, and rhodamine based on the type of the substituents on the 3- and 6-position [16]. They are well known because of their switchable fluorescent off–on flexibility. Xanthene dyes can produce fluorescence wavelengths above 510 nm, reaching far-red areas depending on the conjugative substituents. Thus, they are of widespread use in optical diagnostic research [17].

The triggers of $ONOO^-$-responsive probes with xanthene as a fluorophore core were generally built on (1) oxidation of the hydrazide (**Xan1–Xan15**) [18][19][20][21][22][23][24][25][26][27][28][29][30][31][32], (2) oxidative cleavage of the substituents at the hydroxyl or amino group (**Xan 16–Xan 28**) [33][34][35][36][37][38][39][40][41][42][43][44][45], (3) oxidation of pyrylium (**Xan 29–Xan 33**) [46][47][48][49][50], and (4) oxidation of the hydrogenated xanthene (**Xan 34–Xan 37**) [51][52][53][54] and others (**Xan 38–Xan 41**) [55][56][57][58].

2.1.1. Hydrazide Oxidative Xanthene Probes

In 2002, Guo et al. reported a spiro form hydrazide rhodamine (**Xan 1**) [18] as the $ONOO^-$ fluorescent probe. The hydrazide probe was colorless and non-fluorescent. Upon treating with $ONOO^-$, the spiro hydrazide group was oxidized, releasing a highly fluorescent rhodamine B. The response finished in as fast as 30 s. Meanwhile, the detection limit was only 24 nM. The response avoids interference from the 10^{-5} M Cu(II) ion. Thus, it represents the rapid, sensitive, and specific fluorescent detection of $ONOO^-$.

Based on the recognized pattern and the easy structurally modification character of rhodamine, a series of related probes were developed, aiming to improve the performance of different aspects of the response (**Figure 1**). Longer emissive wavelengths (up to the NIR range) were obtained with more conjugate groups installed in **Xan 2–5** [19][20]

[21][22], **Xan 8** [25], and **Xan 10** [27]. Dual-channel fluorescence was afforded when coumarins were introduced to the rhodamine ring (515/700 nm for **Xan 5** and 631/669 nm for **Xan 10**), making the response produce more information. Ratiometric fluorescence was realized in **Xan 6** [23] and **Xan 7** [24] with the introduction of a 2-(2′-hydroxyphenyl)benzothiazole group and a 4-hydroxycarbazole group, respectively, in which the intensity of the original band disappeared with the generation of a new band with a longer wavelength. Large Stokes shift and excellent lysosome-targeting ability were achieved with the engineering of a fused tetrahydroquinoxaline ring, making **Xan 9** [26] capable of detecting both peroxynitrite and lysosomal pH. Sodium-dependent multivitamin transporter (SMVT)-targeted ability was acquired by introducing the biotin group for Xan 9, making it possible to detect the peroxynitrite in head and neck cancer cells.

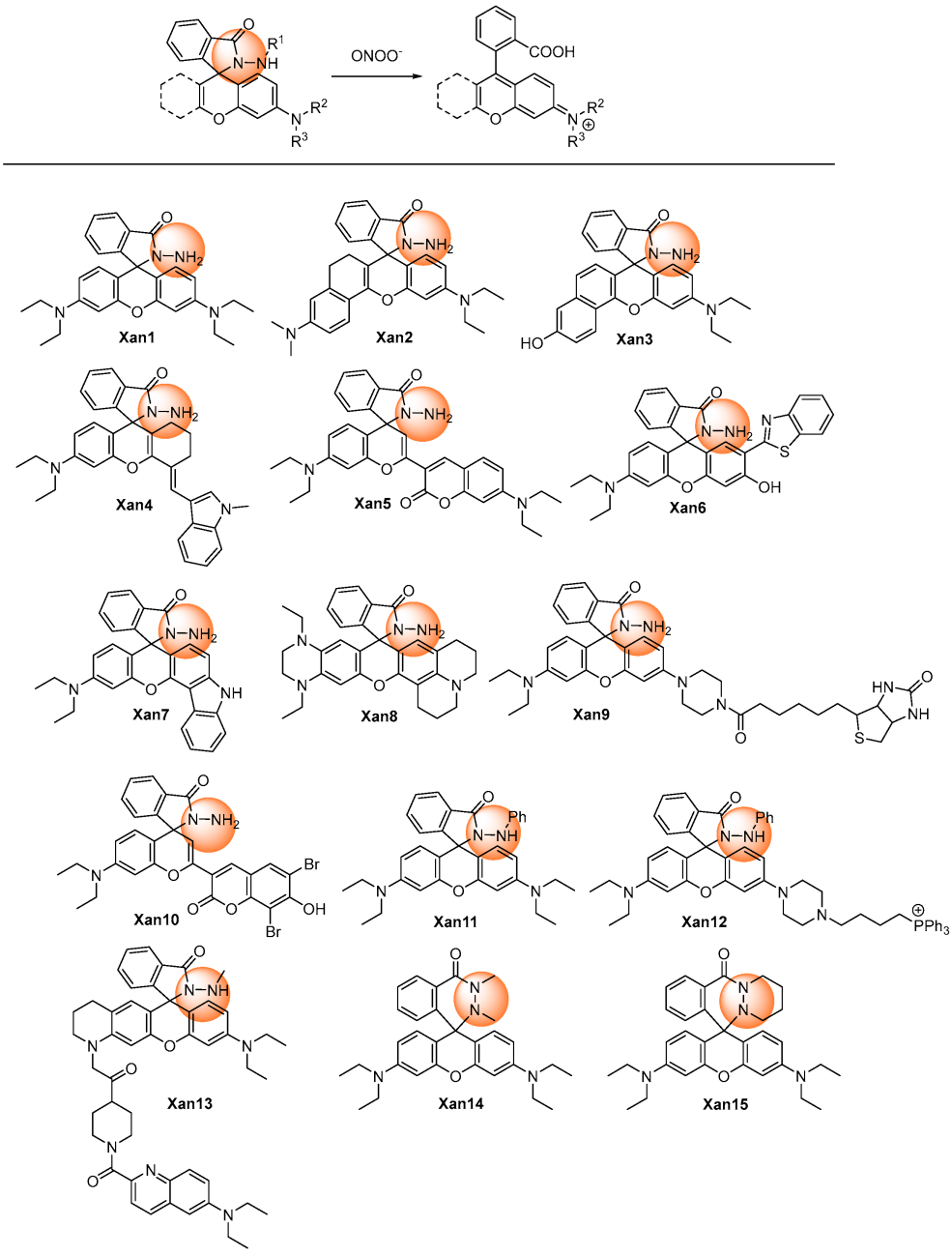

Figure 1. Chemical structures of the hydrazide oxidative xanthene probes.

If a phenyl group was introduced into the hydrazide (**Xan 11–Xan 12**) [28][29], the response time would prolong to 10 or more minutes, presumably due to the steric-hindrance-caused decreased reactivity. It should be noted that, with alkyl substituent groups in both nitrogens of the hydrazide, the cyclic hexahydropyridazin probes (**Xan 14–Xan 15**) [31][32] displayed a faster response rate than the alkyl-substituted (**Xan 13**) [30] or phenyl substituted hydrazide xanthene (**Xan 11–Xan 12**). The response was usually specific, without interferences from a lot of metal ions and other reactive oxygen and nitrogen species. [28][29][30][31][32]

Peroxynitrite generated from different cells, such as HeLa, RAW264.7, HepG2, HSC-2, and Cal-27, could be detected by hydrazide xanthenes. Meanwhile, these probes could detect peroxynitrite in zebrafish and mouse models. These outstanding performances made hydrazide xanthenes capable of revealing the important roles of peroxynitrite in many kinds of diseases, such as respiratory infectious diseases and inflammation in the future.

2.1.2. Oxidative Cleavage of the Recognition Groups to Release Xanthene Probes

Utilizing the oxidative ability of peroxynitrite, the recognition groups at the 2- or 6-hydroxyl or amino group of xanthenes derivative could be cleaved to release xanthenes with high fluorescence (**Figure 2**).

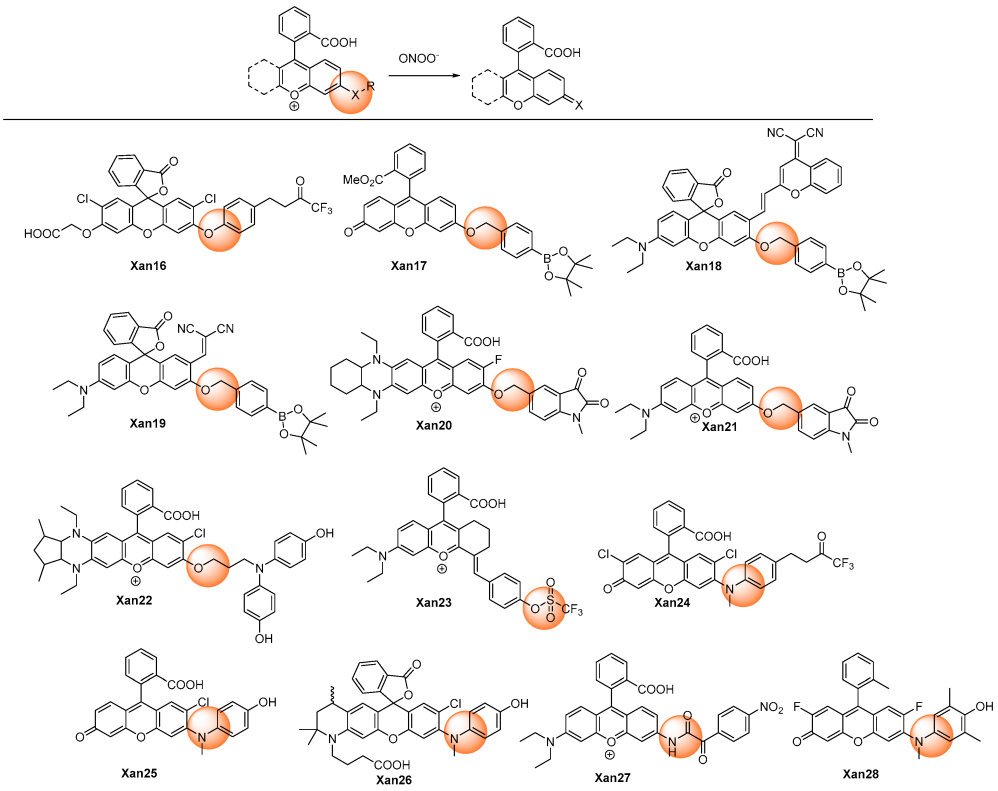

Figure 2. Chemical structures of the oxidative cleavage xanthene probes.

Yang et al. developed the HKGreen series of rhodamine probes (**Xan 16** [33] and **Xan 24** [41]) for detecting peroxynitrite with the employment of the trifluoromethyl ketone as the recognition group, which involved dioxirane rearrangement and oxidative O- or N-diarylation. The response was highly selective and sensitive, with high-fold fluorescent enhancement, though the response time was relatively long (>15 min).

While using the benzyl boronates moiety as a recognition group, **Xan 17–19** [33][34][35] exhibited quite different responsive behaviors upon reactive species. **Xan 17** [33] reacted not only to peroxynitrite but also with hypochlorite and hydrogen peroxide, though with different second-order rate constants. However, **Xan 18** [34] and **Xan 19** [35] responded exclusively to peroxynitrite, even when hypochlorite and hydrogen peroxide were at much higher concentrations. Nevertheless, all of them displayed obvious fluorescent enhancement and low detection limits, and thus they were all further employed for fluorescent imaging in biosystems involving diseases such as drug-introduced liver injury.

The 1-methylindoline-2,3-dione group can also be employed as the recognition moiety for the specific detection of peroxynitrite (**Xan 20** [36] and **Xan 21** [37]). The mechanism involving intramolecular cyclization of peroxynitrite with indoline-2,3-dione, rearrangement, and 1,6-elimination was proposed [36]. Leveraging the probes, the two-photon (TP) in vivo NIR imaging technique was applied to observe the peroxynitrite level in a mouse tumor, a tumor onset on the second day, a kidney injury of zebrafish, and the microvessels of mouse brains with strokes [37].

Xanthenes with the electron-donating groups substituted phenyl groups as recognition groups (**Xan 16** [33], **Xan 24** [41], **Xan 25** [42], **Xan 26** [43], and **Xan 28** [45]) produced very high fluorescent enhancement, probably due to their better quenching effect.

2.1.3. Oxidation of Pyrylium

Yuan et al. discovered an aminophenyl-substituted pyrylium as a highly sensitive and selective scaffold towards peroxynitrite after the screening of nineteen dyes and then further modified it to a FRET probe (**Xan 29**) [46] with TP absorption. After the response, the pyrylium emission band at 651 nm disappeared, and a coumarin characteristic emission band at 473 nm was enhanced. Detailed response mechanisms involving nucleophilic addition, oxidation, elimination, and hydrolysis reactions on chromenylium fluorophore were proposed and verified by MS spectra. Although the destroyed-type response led to the decrease of the emission wavelength, the combination technique of the ratiometric measure and TP imaging made it possible to specifically and rapidly visualize the peroxynitrite in an inflamed mouse model. Furthermore, the detection limit was as low as 11.3 nM, which was at a super level among the peroxynitrite probes. Subsequently, similar structures were synthesized for different applications. Gong et al. reported esterified **Xan 30** [47] with better membrane penetrability and mitochondria targeting ability, which could image the peroxynitrite in the acute liver injury model in living cells. Li et al. introduced a piperazine ring to respond to the pH and finally realized the fluorescent imaging of the cellular peroxynitrite level as well as the mitophagy behavior [48].

Yuan et al. performed an original structure–activity relationship study of the substituents at the recognition site. (**Figure 3**) They discovered that pyrylium involving aryl substituents with strong electron-withdrawing groups could improve the sensitivity; meanwhile, pyrylium involving aryl substituents with strong electron-donating groups could improve the selectivity. Hence, they designed a coumarin, which was a not strong electron-withdrawing and -donating group, substituted pyrylium (**Xan 32**) [49] to satisfy the high requirements of both selectivity and sensitivity, and the results showed that an outstanding detection sensitivity of 4.1 nM of the detection limit as well as a high

130-fold ratiometric emission signal were realized. Employing the probe, the changing content of peroxynitrite in the diseases model involving nonalcoholic fatty liver and drug-induced liver injury was successfully visualized to unfold the functionality of a related enzyme. Zhou et al. introduced a naphthimide fluorophore in the xanthene carboxylic position. After the response, both coumarin and naphthimide fluorescence were produced to output a multicolor signal. The probe **Xan 33** was applied for the early detection and evaluation of arthritis [50].

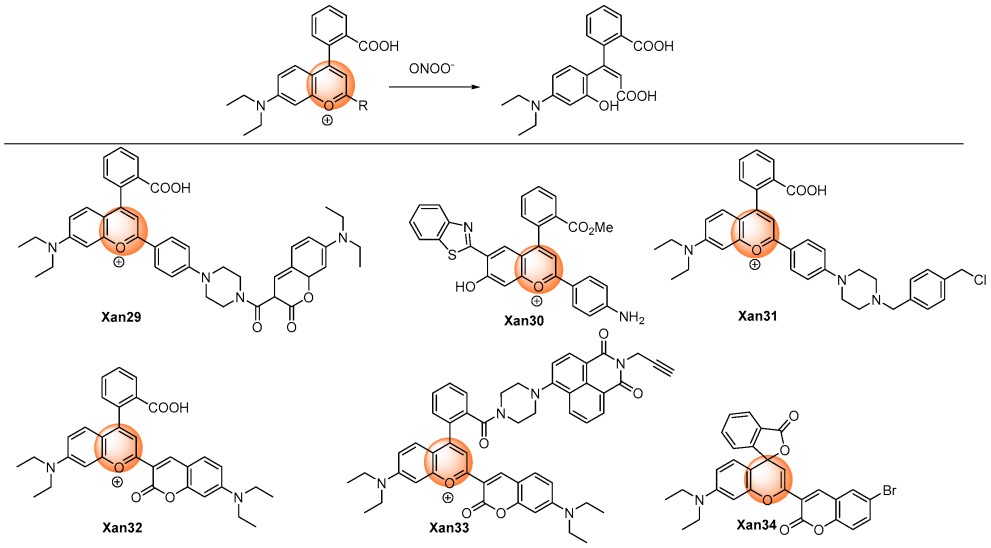

Figure 3. Chemical structures of the pyrylium oxidative xanthene probes.

However, a similar structure–activity relationship study conducted by Tang et al. produced totally different results and response mechanisms, in which electron-withdrawing groups were installed in the 6-position of coumarin moiety. They found that because of the installation of the electron-withdrawing groups in the 6-position of coumarin, **Xan 34** produced 4-(2-carboxylphenyl)-7-diethylaminocoumarin (λem = 520 nm) and 3-hydroxy-6-bromocoumarin (non-fluorescent) as products after the response [51]; nevertheless, **Xan 32** and **Xan 33** produced 3-carboxyl-7-diethylaminocoumarin (λem = ~468 nm) and a ring-opening product of pyrylium (non-fluorescent). Furthermore, **Xan 34** could also detect biothiols by the additional recognition site on coumarin.

2.1.4. Oxidation of Hydrogenated Xanthene

Peroxynitrite can oxidize t non-fluorescent hydrogenated xanthene to produce highly fluorescent aromatic products. (**Figure 4**) Gong et al. developed 9,10-dihydroacridine **Xan 35** as the peroxynitrite detection probe. An over 100-fold fluorescence enhancement could be achieved after reacting with peroxynitrite. The probe was utilized to detect intracellular peroxynitrite [52]. Similar O-, Si-, and P- hydrogenated rhodamine systems were also reported. **Xan 36–37** [53][54] displayed a very fast response speed (<20 s); for **Xan 38** [55], the relatively low response speed was probably due to the low reactivity caused by the presence of the electron-withdrawing phosphonic group. Nevertheless, **Xan 35–38** [52][53][54][55] all exhibited very low detection limits at the nanomolar level, and they were all applied to fluorescent imaging of cell endogenous peroxynitrite.

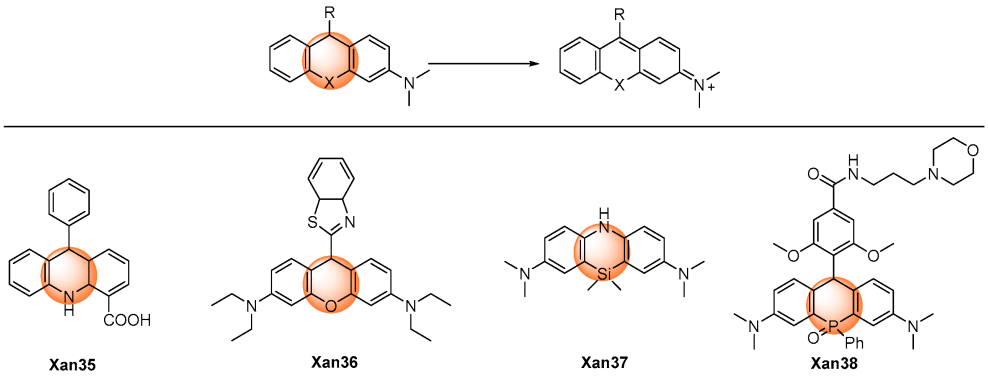

Figure 4. Chemical structures of the oxidative hydrogenated xanthene probes.

2.1.5. Others

Wu et al. described a Rhodol-based probe, **Xan 39** [56], which introduced 1,1-dimethylhydrazone as a peroxynitrite recognition group. (**Figure 5**) The probe was non-fluorescent as a result of the rotational vibration of the C=N bond. Using the oxidative ability of peroxynitrite, the hydrazine was oxidatively cleaved into the corresponding aldehyde with significant fluorescence. The response exhibited a low detection limit (57 nM) with a short response time (<60 s). The probe was applied in the fluorescent imaging of exogenous and endogenous peroxynitrite in living cells.

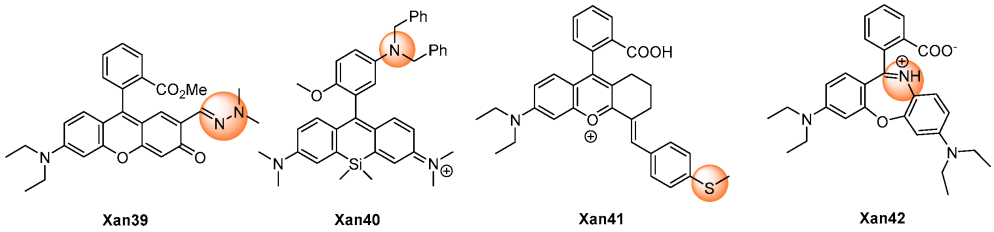

Figure 5. Chemical structures of the other xanthene probes.

Miao et al. reported **Xan 40** [57] as a peroxynitrite off–on probe. The probe showed little fluorescence because of the photo-induced electron transfer (PeT) quenching effect of the 3-dibenzylaminophenyl group. Upon reaction with peroxynitrite, a benzyl group was removed and formed an N-oxide product, and the fluorescent was turned on.

Li et al. released the study on **Xan 41** [58] as a peroxynitrite probe, in which the fluorescence was turned off by the intramolecular charge transfer (ICT) effect of the 4-methylthiophenyl group. After the response with peroxynitrite, the thiol ether was transformed into sulfoxide and discontinued the ICT effect, thus recovering the fluorescence and realizing the detection of the peroxynitrite concentration.

Zhang et al. reported a novel rhodamine probe **Xan 42** with the dibenzo[1,4]oxazepine core as the responsive moiety [59]. Synthesized by the reaction of rhodamine with hydroxylamine, the probe was of little fluorescence at 672 nm. However, after the treatment with peroxynitrite, oxazines was generated with high fluorescence. The probe was used to monitor the peroxynitrite level in living cells.

2.2. Dicyano-Based Compounds as Fluorophore Core

Dicyano-based compounds are characteristic of their donor–π–acceptor structure, which endows them with large Stokes shifts and excellent photostability as a result of the ICT process. In addition, this sort of chromophore was generally easily synthesized and structurally modified. Thus, great attention has been attracted towards dicyano-based compounds to build probes with different functionalities [60].

The designing rule for dicyano-based peroxynitrite probes was a consensus, which was described in **Figure 6**. In general, the responsive groups, such as diphenylphosphonyl, benzyl boronates, and 4-hydroxyphenyl, were modified on the donor moiety to stop the ICT process. The response with peroxynitrite would break the links between the donor moiety and the response groups and release the dicyano-based chromophores with strong fluorescence.

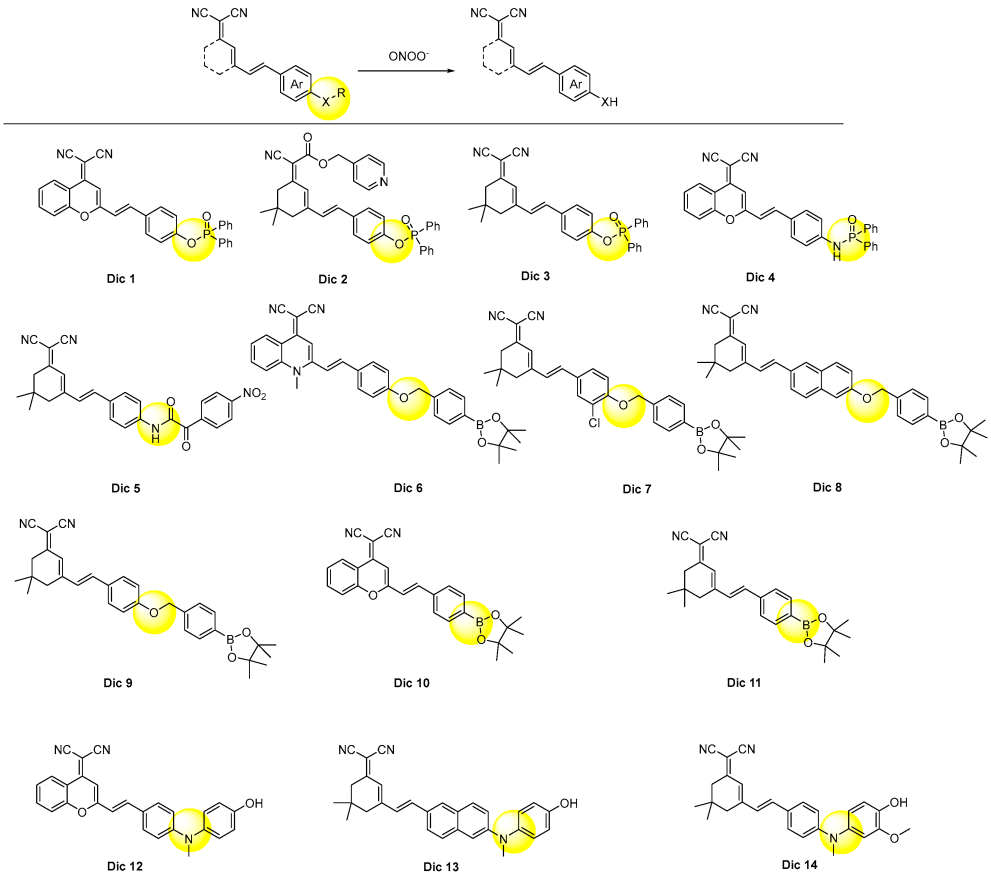

Figure 6. Chemical structures of the dicyano-based probes.

As summarized in **Table 1**, **Dic 1–4** [61][62][63][64], with diphenylphosphonyl as a recognition group, took more than 10 min to respond, which was relatively longer than those of **Dic 5–14** [65][66][67][68][69][70][71][72][73][74]. This was probably due to their high intrinsic structural stability. However, their detection selectivity and sensitivity were not reduced. Thus, they were employed for fluorescent imaging of the exogenous peroxynitrite in living cells. Among them, **Dic 4** were further used to manifest the changing peroxynitrite concentration in the rat epilepsy model with the aid of two-photon fluorescent technology [64].

Dic 5 [65] with the 4-nitrophenyl oxoacetyl group as the responsive unit showed a much faster response rate (<2 s) than **Dic 1–4**, but its detection limit was at a similar level (81 nM). The probe was used for fluorescence imaging of the endogenous peroxynitrite in zebrafish and mice.

All of the benzyl boronates derived dicyano-based probes **Dic 6–10** showed analogous response times to each other. Interestingly, **Dic 6** [66] and **Dic 10** [70] only displayed green-channel fluorescence, although they both have an extra conjugate phenyl ring compared **Dic 7** [67] and **Dic 9** [69], respectively. The boronate group of **Dic 10–11** was oxidized to the hydroxyl group in situ by peroxynitrite, and the transformation generated the donor, thus forming the ICT process and producing fluorescence.

The response rates of the probes **Dic 12–14** [72][73][74], which employed 4-hydroxylphenyl as a masking group, were all found to be ultrafast, which were 5, 25, and 1 s, respectively. This phenomenon was in accordance with those of **Xan 25–26** [42][43] and **Xan 28** [45], suggesting the great advantage of this mask group. Possessing the superior detecting sensitivity and selectivity, the probes **Dic 12–14** were applied to visualize the peroxynitrite in different diseases, including inflammation, acute liver injury, and Parkinson's disease [72][73][74].

2.3. Coumarin as Fluorophore Core

The research history of coumarin (also known as 1-benzopyran-2-one or 2H-chromen-2-one) was more than 200 years. Plenty of extensive investigations have been performed to modify the weak fluorescent parent coumarin to its derivatives with different desired photophysical properties, with a considerable amount of them now very active in the commercial market [75].

Inserting the electron-donors in the 7-position leads to a bathochromic shift to the emission wavelength; in addition, a donor–π–donor structure was formed, which facilitates the use of itself to design the ICT type probes by further introducing an electron-acceptor recognition group. (**Figure 7**) Xie et al. adopted this strategy and synthesized **Cou 1** [76]. The 4-nitrophenyl oxoacetyl recognition group reacted with peroxynitrite rapidly and produced the deprotected product **Cou 2** [77]. They used **Cou 1**, together with the two-photon fluorescent imaging technology, to visualize the peroxynitrite produced in the mitochondria in an anthracycline-induced cardiotoxicity mouse model. However, Li et al. reported that the deprotected product, **Cou 2**, also further reacted with peroxynitrite in 5 s in the concentration range of 0.064–0.64 μM, and the resulting nitration products were confirmed by ESI-MS analysis. The 3-position of coumarin could also be introduced with electron-donors to generate the donor–π–donor structure. Wei et al. developed **Cou 3** as the peroxynitrite probe using the 4-nitrophenyl oxoacetyl group as a recognition moiety [78]. The fluorescence of **Cou 3** was quenched but could be quickly recovered with eight-fold enhancement after the response with peroxynitrite. The probe was used to image exogenous peroxynitrite formation in living cells in a biosystem.

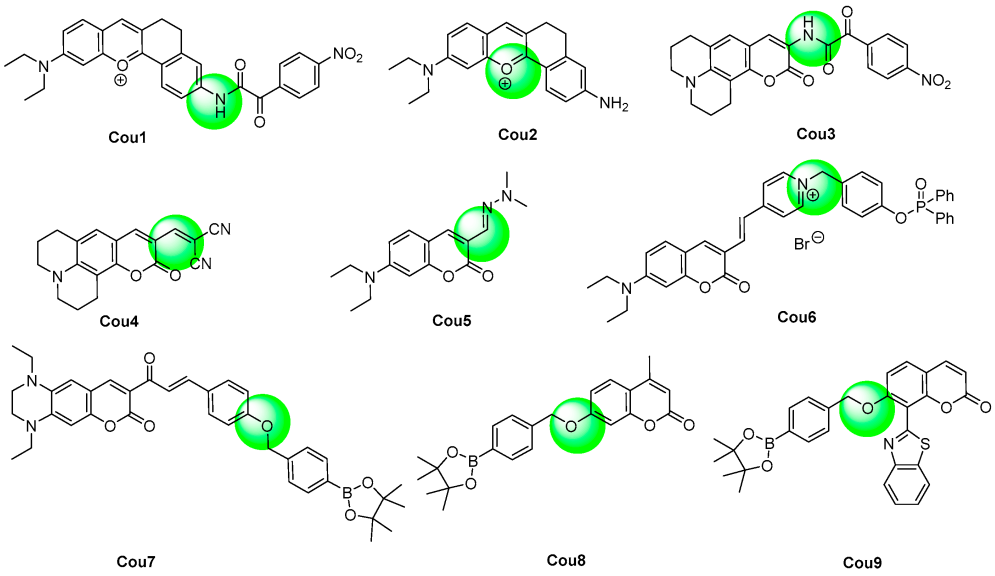

Figure 7. Chemical structures of the coumarin probes.

The electron effect of the substituents of the 3-position of 7-dialkylaminocoumarin derivatives decided their emission properties. The existence of an electron-acceptor can cause a strong ICT effect and fluorescence, and the stronger the electron-withdrawing ability the group owned, the longer the emission wavelength and stronger fluorescence the probes owned. If the electron-withdrawing ability changed, the fluorescent property would change accordingly. For example, the formyl group is a medium-ability electron-withdrawing group. If it was transformed into stronger electron-withdrawing groups, the emission wavelength of the product, **Cou 4**, would increase [79]. In reverse, after the response with peroxynitrite, the C=C bond of **Cou 4** broke and generated the aldehyde product. The response was completed in a very short time with high selectivity and sensitivity to peroxynitrite. If the aldehyde group was reacted with hydrazine, the hydrazone product **Cou 5** would emit only little fluorescence. However, after the reaction with peroxynitrite, the fluorescence would recover [80].

The ICT process is very strong in the quaternized pyridinium probe **Cou 6** [81]. After the addition of peroxynitrite, the diphenyl phosphinate was eliminated, and the product owned a very weak ICT process. The fluorescence undergoes a hypochromatic shift from 643 nm to 538 nm, and the emission ration displays a 153-fold increase. The probe was applied to detect the peroxynitrite in living cells.

Parthiban et al. reported a coumarin–chalcone hybrid peroxynitrite probe **Cou 7** containing a tetrahydroquinoxaline ring [82]. The probe displayed a large Stokes shift of 149 nm. The aryl boronate group was employed as the recognition group for peroxynitrite. The probe exhibited exceptional speed and sensitivity in detecting peroxynitrite. Palanisamy described another coumarin probe **Cou 8** with a 7-position aryl boronate group as the response moiety, and the probe was applied to fluorescence imaging of peroxynitrite in a high-fat diet-induced obese mouse model [83].

Wang et al. reported a coumarin probe **Cou 9**-based 7-position benzyl borate as a recognition group. The probe exhibited weak ICT and weak fluorescence at 421 nm [84]. After the reaction with peroxnitrie, a strong ICT and

FRET process was turned on and led to an incredible 1200-fold enhancement of the fluorescence. The probe was used for fluorescent imaging of the content of peroxnitrie in cancer cells.

2.4. N-Substituted Coumarin as Fluorophore Core

As analogues for coumarin dyes, 2-(benzo[d]thiazol-2-yl)phenylacrylonitrile derivatives exhibited longer emission wavelengths than the related coumarins. (**Figure 8**) In particular, 2-(benzo[d]thiazol-2-yl)-3-(2-hydroxyphenyl)acrylonitrile derivatives (**NCou 1–3**) [85][86][87] served as the precursors for iminocoumarin, and they exhibited aggregation-induced emission luminogens (AIEgens) in aqueous conditions. Upon the response with peroxynitrite, 2-(benzo[d]thiazol-2-yl)-3-(2-hydroxyphenyl)acrylonitrile would be generated, which would further transform into iminocoumarin in situ. The probes were applied for the fluorescent imaging of cell exogenous and endogenous peroxynitrite, though the response rate was usually relatively slow.

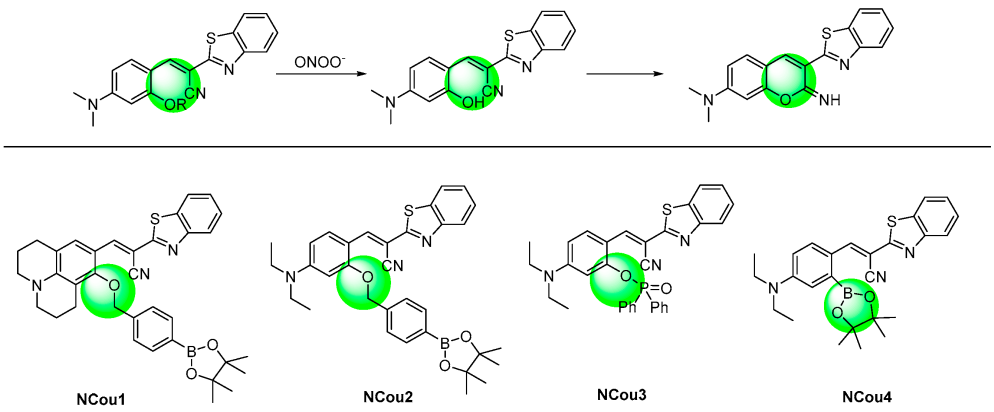

Figure 8. Chemical structures of the N-substituted coumarin probes and their responsive mechanism.

The hydroxyl group was also converted from the borate group. The probe **NCou 4** exhibited high speed and sensitivity in detecting peroxynitrite [88]. The detection limit of the probe for peroxynitrite was 0.83 nM.

References

1. Radi, R. Peroxynitrite, a Stealthy Biological Oxidant. J. Biol. Chem. 2013, 288, 26464–26472.
2. Radi, R.; Beckman, J.S.; Bush, K.M.; Freeman, B.A. Peroxynitrite oxidation of sulfhydryls. The cytotoxic potential of superoxide and nitric oxide. J. Biol. Chem. 1991, 266, 4244–4250.
3. Ducrocq, C.; Blanchard, B.; Pignatelli, B.; Ohshima, H. Peroxynitrite: An endogenous oxidizing and nitrating agent. Cell. Mol. Life Sci. 1999, 55, 1068–1077.
4. Masumoto, H.; Kissner, R.; Koppenol, W.H.; Sies, H. Kinetic study of the reaction of ebselen with peroxynitrite. FEBS Lett. 1996, 398, 179–182.

5. Butler, A.R.; Feelisch, M. Therapeutic uses of inorganic nitrite and nitrate: From the past to the future. Circulation 2008, 117, 2151–2159.
6. Singh, D.K.; Winocour, P.; Farrington, K. Oxidative stress in early diabetic nerphropathy: Fueling the fire. Nat. Rev. Endocrinol. 2011, 7, 176–184.
7. Migita, K.; Yamasaki, S.; Ida, H.; Kita, M.; Hida, A.; Shibatomi, K.; Kawakami, A.; Aoyagi, T.; Eguchi, K. The role of peroxynitrite in cyclooxygenase-2 expression of rheumatoid synovium. Clin. Exp. Rheumatol. 2002, 20, 59–62.
8. Mahdi, A.; Tengbom, J.; Alvarsson, M.; Wernly, B.; Zhou, Z.; Pernow, J. Red Blood Cell Peroxynitrite Causes Endothelial Dysfunction in Type 2 Diabetes Mellitus via Arginase. Cells 2020, 9, 1712.
9. Pandey, V.K.; Amin, P.J.; Shankar, B.S. G1-4A, a polysaccharide from Tinospora cordifolia induces peroxynitrite dependent killer dendritic cell (KDC) activity against tumor cells. Int. Immunopharmacol. 2014, 23, 480–488.
10. Vana, L.; Kanaan, N.M.; Hakala, K.; Weintraub, S.T.; Binder, L.I. Peroxynitrite-induced nitrative and oxidative modifications alter tau filament formation. Biochemistry 2011, 50, 1203–1212.
11. Tarpey, M.M.; Fridovich, I. Methods of detection of vascular reactive species: Nitric oxide, superoxide, hydrogen peroxide, and peroxynitrite. Circ. Res. 2001, 89, 224–236.
12. Ma, Q.; Xu, S.; Zhai, Z.; Wang, K.; Liu, X.; Xiao, H.; Zhuo, S.; Liu, Y. Recent Progress of Small-Molecule Ratiometric Fluorescent Probes for Peroxynitrite in Biological Systems. Chem. Eur. J. 2022, 28, e202200828.
13. Wang, S.; Chen, L.; Jangili, P.; Sharma, A.; Li, W.; Hou, J.T.; Qin, C.; Yong, J.; Kim, J.S. Design and applications of fluorescent detectors for peroxynitrite. Coord. Chem. Rev. 2018, 374, 36–54.
14. Mao, Z.; Xiong, J.; Wang, P.; An, J.; Zhang, F.; Liu, Z.; Kim, J.S. Activity-based fluorescence probes for pathophysiological peroxynitrite fluxes. Coord. Chem. Rev. 2022, 454, 214356.
15. Cui, W.-L.; Wang, M.-H.; Yang, Y.-H.; Wang, J.-Y.; Zhu, X.; Zhang, H.; Ji, X. Recent advances and perspectives in reaction-based fluorescent probes for imaging peroxynitrite in Biological Systems. Coord. Chem. Rev. 2023, 474, 214848.
16. Khan, Z.; Sekar, N. Far-red to NIR emitting xanthene-based fluorophores. Dye. Pigment. 2022, 208, 110735.
17. Poronik, Y.M.; Vygranenko, K.V.; Gryko, D.; Gryko, D.T. Rhodols—Synthesis, photophysical properties and applications as fluorescent probes. Chem. Soc. Rev. 2019, 48, 5242–5265.
18. Yang, X.F.; Guo, X.Q.; Zhao, Y.B. Development of a novel rhodamine-type fluorescent probe to determine peroxynitrite. Talanta 2002, 57, 883–890.

19. Wu, D.; Ryu, J.C.; Chung, Y.W.; Lee, D.; Ryu, J.H.; Yoon, J.H.; Yoon, J. A Far-Red-Emitting Fluorescence Probe for Sensitive and Selective Detection of Peroxynitrite in Live Cells and Tissues. Anal. Chem. 2017, 89, 10924–10931.
20. Zhu, B.C.; Zhang, M.; Wu, L.; Zhao, Z.Y.; Liu, C.Y.; Wang, Z.K.; Duan, Q.X.; Wang, Y.W.; Jia, P. A highly specific far-red fluorescent probe for imaging endogenous peroxynitrite in the mitochondria of living cells. Sens. Actuators B Chem. 2018, 257, 436–441.
21. Liu, D.; Feng, S.; Feng, G. A rapid responsive colorimetric and near-infrared fluorescent turn-on probe for imaging exogenous and endogenous peroxynitrite in living cells. Sens. Actuators B Chem. 2018, 269, 15–21.
22. Feng, S.M.; Liu, D.D.; Feng, G.Q. A dual-channel probe with green and near-infrared fluorescence changes for invitro and invivo detection of peroxynitrite. Anal. Chim. Acta 2019, 1054, 137–144.
23. Jia, P.; Zhuang, Z.H.; Liu, C.Y.; Wang, Z.K.; Duan, Q.X.; Li, Z.L.; Zhu, H.C.; Zhang, F.F.; Sheng, W.L.; Zhu, B.C. Development of a ratiometric fluorescent probe with a large emission shift for imaging ONOO− in live cells and zebrafish. Dye. Pigment. 2020, 173, 107942.
24. Ding, H.Y.; Peng, L.P.; Yuan, G.Q.; Zhou, L.Y. Design, synthesis and bioimaging application of a novel two-photon xanthene fluorescence probe for ratiometric visualization of endogenous peroxynitrite in living cells and zebrafish. Dye. Pigment. 2020, 176, 108232.
25. Xia, Q.F.; Feng, S.M.; Hong, J.X.; Feng, G.Q. One probe for multiple targets: A NIR fluorescent rhodamine-based probe for ONOO− and lysosomal pH detection in live cells. Sens. Actuators B Chem. 2021, 337, 129732.
26. Wu, Y.; Zhang, X.; Lu, X.Y.; Chen, Y.; Ju, J.D.; Wu, H.W.; Zhu, B.C.; Huang, S.Y. An SMVT-targeting and peroxynitrite-activating fluorescent probe for head and neck cancer imaging and peroxynitrite detection. Sens. Actuators B Chem. 2021, 348, 130677.
27. Huang, W.M.; Du, X.M.; Zhang, C.J.; Zhang, S.R.; Zhang, J.J.; Yang, X.F. Rational Design of a Dual-Channel Fluorescent Probe for the Simultaneous Imaging of Hypochlorous Acid and Peroxynitrite in Living Organisms. Anal. Chem. 2022, 94, 17485–17493.
28. Ambikapathi, G.; Kempahanumakkagari, S.K.; Lamani, B.R.; Shivanna, D.K.; Maregowda, H.B.; Gupta, A.; Malingappa, P. Bioimaging of Peroxynitrite in MCF-7 Cells by a New Fluorescent Probe Rhodamine B Phenyl Hydrazide. J. Fluoresc. 2013, 23, 705–712.
29. Li, H.Y.; Li, X.H.; Wu, X.F.; Shi, W.; Ma, H.M. Observation of the Generation of ONOO– in Mitochondria under Various Stimuli with a Sensitive Fluorescence Probe. Anal. Chem. 2017, 89, 5519–5525.
30. Chen, S.Y.; Vurusaner, B.; Pena, S.; Thu, C.T.; Mahal, L.K.; Fisher, E.A.; Canary, J.W. Two-Photon, Ratiometric, Quantitative Fluorescent Probe Reveals Fluctuation of Peroxynitrite Regulated by Arginase 1. Anal. Chem. 2021, 93, 10090–10098.

31. Liu, C.Y.; Zhang, X.; Li, Z.L.; Chen, Y.N.; Zhuang, Z.H.; Jia, P.; Zhu, H.C.; Yu, Y.M.; Zhu, B.C.; Sheng, W.L. Novel Dimethylhydrazine-Derived Spirolactam Fluorescent Chemodosimeter for Tracing Basal Peroxynitrite in Live Cells and Zebrafish. J. Agric. Food Chem. 2019, 67, 6407–6413.
32. Zhang, X.; Chen, Y.N.; Liu, C.Y.; Zhuang, Z.H.; Li, Z.; Jia, P.; Zhu, H.C.; Yu, Y.M.; Zhu, B.C.; Sheng, W. A novel hexahydropyridazin-modified rhodamine fluorescent probe for tracing endogenous/exogenous peroxynitrite in live cells and zebrafish. Dye. Pigment. 2019, 170, 107573.
33. Yang, D.; Wang, H.L.; Sun, Z.N.; Chung, N.W.; Shen, J.G. A Highly Selective Fluorescent Probe for the Detection and Imaging of Peroxynitrite in Living Cells. J. Am. Chem. Soc. 2006, 128, 6004–6005.
34. Dębowska, K.; Dębski, D.; Michałowski, B.; Dybala-Defratyka, A.; Wójcik, T.; Michalski, R.; Jakubowska, M.; Selmi, A.; Smulik, R.; Piotrowski, Ł.; et al. Characterization of Fluorescein-Based Monoboronate Probe and Its Application to the Detection of Peroxynitrite in Endothelial Cells Treated with Doxorubicin. Chem. Res. Toxicol. 2016, 29, 735–746.
35. Wen, L.; Ma, X.Y.; Yang, J.; Jiang, M.M.; Peng, C.; Ma, Z.Y.; Yu, H.; Li, Y.H. A New Ratiometric Design Strategy Based on Modulation of π-Conjugation Unit for Developing Fluorescent Probe and Imaging of Cellular Peroxynitrite. Anal. Chem. 2022, 94, 4763–4769.
36. Peng, C.; Yang, J.F.; Li, W.; Lin, D.; Fei, Y.X.; Chen, X.L.; Yuan, L.; Li, Y.H. Development of Probes with High Signal-to-Noise Ratios Based on the Facile Modification of Xanthene Dyes for Imaging Peroxynitrite during the Liver Ischemia/Reperfusion Process. Anal. Chem. 2022, 94, 10773–10780.
37. Wang, W.W.; Xiong, J.H.; Song, X.J.; Wang, Z.; Zhang, F.; Mao, Z.Q. Activatable Two-Photon Near-Infrared Fluorescent Probe Tailored toward Peroxynitrite In Vivo Imaging in Tumors. Anal. Chem. 2020, 92, 13305–13312.
38. Xiong, J.H.; Wang, W.W.; Wang, C.X.; Zhong, C.; Ruan, R.Q.; Mao, Z.Q.; Liu, Z.H. Visualizing Peroxynitrite in Microvessels of the Brain with Stroke Using an Engineered Highly Specific Fluorescent Probe. ACS Sens. 2020, 5, 3237–3245.
39. Wang, P.Z.; Yu, L.; Gong, J.K.; Xiong, J.H.; Zi, S.Y.; Xie, H.; Zhang, F.; Mao, Z.Q.; Liu, Z.H.; Kim, J.S. An Activity-Based Fluorescent Probe for Imaging Fluctuations of Peroxynitrite (ONOO−) in the Alzheimer’s Disease Brain. Angew. Chem. 2022, 61, e202206894.
40. Shi, A.; Zeng, Y.L.; Xin, D.X.; Zhou, Y.Y.; Zhao, L.Z.; Peng, J.J. Real-Time Visualization of the Antioxidative Potency of Drugs for the Prevention of Myocardium Ischemia-Reperfusion Injury by a NIR Fluorescent Nanoprobe. ACS Sens. 2022, 7, 3867–3875.

41. Peng, T.; Yang, D. HKGreen-3: A Rhodol-Based Fluorescent Probe for Peroxynitrite. Org. Lett. 2010, 12, 4932–4935.
42. Peng, T.; Wong, N.K.; Chen, X.; Chan, Y.K.; Ho, D.H.H.; Sun, Z.N.; Hu, J.J.; Shen, J.Q.; El-Nezami, H.; Yang, D. Molecular Imaging of Peroxynitrite with HKGreen-4 in Live Cells and Tissues. J. Am. Chem. Soc. 2014, 136, 11728–11734.
43. Peng, T.; Chen, X.M.; Gao, L.; Zhang, T.; Wang, W.; Shen, J.G.; Yang, D. A rationally designed rhodamine-based fluorescent probe for molecular imaging of peroxynitrite in live cells and tissues. Chem. Sci. 2016, 7, 5407–5413.
44. Cheng, D.; Xu, W.; Yuan, L.; Zhang, X.B. Investigation of Drug-Induced Hepatotoxicity and Its Remediation Pathway with Reaction-Based Fluorescent Probes. Anal. Chem. 2017, 89, 7693–7700.
45. Knewtson, K.E.; Rane, D.; Peterson, B.R. Targeting Fluorescent Sensors to Endoplasmic Reticulum Membranes Enables Detection of Peroxynitrite During Cellular Phagocytosis. ACS Chem. Biol. 2018, 13, 2595–2602.
46. Cheng, D.; Pan, Y.; Wang, L.; Zeng, Z.B.; Yuan, L.; Zhang, X.B.; Chang, Y.T. Selective Visualization of the Endogenous Peroxynitrite in an Inflamed Mouse Model by a Mitochondria-Targetable Two-Photon Ratiometric Fluorescent Probe. J. Am. Chem. Soc. 2017, 139, 285–292.
47. Gong, X.Y.; Cheng, D.; Li, W.; Shen, Y.; Peng, R.; Shi, L.W.; He, L.; Yuan, L. A highly selective ratiometric molecular probe for imaging peroxynitrite during drug-induced acute liver injury. J. Mater. Chem. B 2021, 9, 8246–8252.
48. Li, M.L.; Huang, Y.; Song, S.M.; Shuang, S.M.; Dong, C. Piperazine-Based Mitochondria-Immobilized pH Fluorescent Probe for Imaging Endogenous ONOO– and Real-Time Tracking of Mitophagy. ACS Appl. Bio Mater. 2022, 5, 2777–2785.
49. Cheng, D.; Gong, X.Y.; Wu, Q.; Yuan, J.; Lv, Y.; Yuan, L.; Zhang, X.B. High-Selectivity Fluorescent Reporter toward Peroxynitrite in a Coexisting Nonalcoholic Fatty Liver and Drug-Induced Liver Diseases Model. Anal. Chem. 2020, 92, 11396–11404.
50. Xu, W.Z.; Yang, Q.M.; Zeng, J.Q.; Tan, L.B.; Zhou, L.Y.; Peng, L.P.; Zhou, Y.Z.; Xie, C.; Luo, K.; Zhang, Z. A biomarker (ONOO−)-activated multicolor fluorescent probe for early detection and assessment of arthritis. Sens. Actuators B Chem. 2022, 359, 131565.
51. Li, Y.; Zhao, Z.W.; Xiao, Y.S.; Wang, X.; Jiao, X.Y.; Xie, X.L.; Zhang, J.; Tang, B. Reactivity Modulation of Benzopyran-Coumarin Platform by Introducing Electron-Withdrawing Groups: Specific Detection of Biothiols and Peroxynitrite. Anal. Chem. 2019, 91, 6097–6102.
52. Li, Z.H.; Liu, R.; Tan, Z.L.; He, L.; Lu, Z.L.; Gong, B. Aromatization of 9,10-Dihydroacridine Derivatives: Discovering a Highly Selective and Rapid-Responding Fluorescent Probe for Peroxynitrite. ACS Sens. 2017, 28, 501–505.

53. Ren, M.H.; Wang, L.F.; Lv, X.; Liu, J.; Chen, H.; Wang, J.J.; Guo, W. Development of a benzothiazole-functionalized red-emission pyronin dye and its dihydro derivative for imaging lysosomal viscosity and tracking endogenous peroxynitrite. J. Mater. Chem. B 2019, 7, 6181–6186.
54. Wang, L.F.; Liu, J.; Zhao, S.W.; Zhang, H.X.; Sun, Y.Q.; Wei, A.; Guo, W. Fluorescence imaging of hypochlorous acid and peroxynitrite in vitro and in vivo with emission wavelength beyond 750 nm. Chem. Commun. 2020, 56, 7718–7721.
55. Lin, X.F.; Fan, M.T.; Li, N.; Yang, J.J.; Zhu, H.D.; Chen, B.; Zhu, J.R.; Zhang, D.Z.; Wang, T.; Cui, X.Y. Phosphorus-substituted rhodamines for bioimaging of the lysosomal peroxynitrite in vivo. Dye. Pigment. 2022, 201, 110201.
56. Wu, J.C.; Lin, Y.F.; Yu, Y.T.; Li, Y.Q.; Ye, T.Q.; Zhou, H.W.; Li, L.; Wang, J.B. A highly selective and sensitive fluorescence probe based on Rhodol for imaging of endogenous peroxynitrite in living cells. Dye. Pigment. 2022, 206, 110597.
57. Miao, J.F.; Huo, Y.Y.; Shi, H.; Fang, J.R.; Wang, J.J.; Guo, W. A Si-rhodamine-based near-infrared fluorescent probe for visualizing endogenous peroxynitrite in living cells, tissues, and animals. J. Mater. Chem. B 2018, 6, 4466–4473.
58. Li, Z.; Lu, J.; Pang, Q.; You, J. Construction of a Near-Infrared Fluorescent Probe for Ratiometric Imaging of Peroxynitrite during Tumor Progression. Analyst 2021, 146, 5204–5211.
59. Zhang, H.; Xu, Y.; Li, H.; Shi, W.; Li, X.; Ma, H. New Rhodamines with Changeable π-Conjugation for Lengthening Fluorescence Wavelengths and Imaging Peroxynitrite. Chem 2022, 8, 287–295.
60. Zhang, W.; Huo, F.; Yin, C. Recent advances of dicyano-based materials in biology and medicine. J. Mater. Chem. B 2018, 6, 6919–6929.
61. Mulay, S.V.; Kim, Y.; Lee, K.J.; Yudhistira, T.; Park, H.S.; Churchill, D.G. A fluorogenic and red-shifted diphenyl phosphinate-based probe for selective peroxynitrite detection as demonstrated in fixed cells. New J. Chem. 2017, 41, 11934–11940.
62. Gu, B.; Liu, C.F.; Wu, Y.; Zhang, C.X.; Shen, Y.M.; Liu, M.Q. Application of a Colorimetric and Near-Infrared Fluorescent Probe in Peroxynitrite Detection and Imaging in Living Cells. ACS Omega 2020, 5, 27530–27535.
63. Zhang, Y.B.; Ma, D.G. Selective detection of peroxynitrite in living cells by a near-infrared diphenyl phosphinate-based dicyanoisophorone probe. Spectrochim. Acta A Mol. Biomol. Spectrosc. 2021, 244, 118890.
64. Luo, X.Z.; Cheng, Z.Y.; Wang, R.; Yu, F.B. Indication of Dynamic Peroxynitrite Fluctuations in the Rat Epilepsy Model with a Near-Infrared Two-Photon Fluorescent Probe. Anal. Chem. 2021, 93, 2490–2499.

65. Yin, X.Y.; Feng, W.Y.; Gong, S.Y.; Feng, G.Q. Near-infrared fluorescent probe with rapid response and large Stokes shift for imaging peroxynitrite in living cells, zebrafish and mice. Dye. Pigment. 2020, 172, 107820.
66. Han, X.J.; Yang, X.P.; Zhang, Y.R.; Li, Z.P.; Cao, W.B.; Zhang, D.; Ye, Y. A novel activatable AIEgen fluorescent probe for peroxynitrite detection and its application in EC1 cells. Sens. Actuators B Chem. 2020, 321, 128510.
67. Kang, H.; Shu, W.; Yu, J.; Gao, M.X.; Han, R.B.; Jing, J.; Zhang, R.B.; Zhang, X.L. A near-infrared fluorescent probe for ratiometric imaging peroxynitrite in Parkinson's disease model. Sens. Actuators B Chem. 2022, 359, 131393.
68. Chen, C.Y.; Yang, Y.S.; Chen, H.; Fan, X.J.; Zhu, H.L.; Li, Z. Imaging pulmonary fibrosis with a practical probe for the detection of peroxynitrite in living cells and mice. Dye. Pigment. 2022, 204, 110443.
69. Xu, J.Q.; Gao, M.J.; Guo, J.S.; Wang, Y.H.; Wei, R.; Meng, Y.L.; Kang, Y.F. A highly selective probe for ratiometric imaging peroxynitrite in living cells and in vivo. Bioorg. Chem. 2022, 128, 106055.
70. Wu, L.L.; Tian, X.; Han, H.H.; Wang, J.; Groleau, R.R.; Tosuwan, P.; Wannalerse, B.; Sedgwick, A.C.; Bull, S.D.; He, X.P.; et al. A Simple Near-Infrared Fluorescent Probe for the Detection of Peroxynitrite. ChemistryOpen 2019, 8, 1407–1409.
71. Jia, P.; Liu, D.M.; Zhuang, Z.H.; Liu, C.Y.; Li, Z.L.; Yu, C.; Chen, Y.N.; Zhu, H.C.; Zhang, X.; Yu, Y.M.; et al. Dicyanoisophorone-Derived Near-Infrared Fluorescent Probe for Ultrasensitive Detection of Peroxynitrite in Living Cells and Zebrafish. Ind. Eng. Chem. Res. 2019, 58, 19778–19784.
72. Zhu, M.Y.; Zhou, H.; Ji, D.D.; Li, G.; Wang, F.; Song, D.Y.; Deng, B.; Li, C.; Qiao, R.Z. A near-infrared fluorescence probe for ultrafast and selective detection of peroxynitrite with large Stokes shift in inflamed mouse models. Dye. Pigment. 2019, 168, 77–83.
73. Jin, C.; Wu, P.F.; Yang, Y.S.; He, Z.X.; Zhu, H.L.; Li, Z. A novel fluorescent probe for the detection of peroxynitrite and its application in acute liver injury model. Redox Biol. 2021, 46, 102068.
74. Sun, Q.; Xu, J.J.; Ji, C.L.; Shaibani, M.S.S.; Li, Z.; Lim, K.; Zhang, C.W.; Li, L.; Liu, Z.P. Ultrafast Detection of Peroxynitrite in Parkinson's Disease Models Using a Near-Infrared Fluorescent Probe. Anal. Chem. 2020, 92, 4038–4045.
75. Cao, D.X.; Liu, Z.Q.; Verwilst, P.; Koo, S.; Jangjili, P.; Kim, J.S.; Lin, W.Y. Coumarin-Based Small-Molecule Fluorescent Chemosensors. Chem. Rev. 2019, 119, 10403–10519.
76. Xie, X.L.; Tang, F.Y.; Liu, G.Z.; Li, Y.; Su, X.X.; Jiao, X.Y.; Wang, X.; Tang, B. Mitochondrial Peroxynitrite Mediation of Anthracycline-Induced Cardiotoxicity as Visualized by a Two-Photon Near-Infrared Fluorescent Probe. Anal. Chem. 2018, 90, 11629–11635.

77. Li, M.L.; Huang, Y.; Song, S.M.; Shuang, S.M.; Wang, R.B.; Dong, C. Sensitive monitoring mitochondrial peroxynitrite based on a new reaction site and cell imaging by anthracycline-based red emitting fluorescence probe. Dye. Pigment. 2021, 195, 109727.
78. Wei, W.P.; Li, R.; Zhu, M.; Zhao, L.L.; Ran, H.Y.; Pang, M.L.; Zhu, G.H. Coumarin-based fluorescence turn-on probes for high selectivity peroxynitrite detection and imaging in living cells and γ-carrageenan-induced inflammatory tissue and mice. Microchem. J. 2022, 183, 108003.
79. Fang, Y.; Chen, R.X.; Qin, H.F.; Wang, J.J.; Zhang, Q.; Chen, S.J.; Wen, Y.H.; Wang, K.P.; Hu, Z.Q. A chromene based fluorescence probe: Accurate detection of peroxynitrite in mitochondria, not elsewhere. Sens. Actuators B Chem. 2021, 334, 129603.
80. Kim, S.; Ko, C.W.; Lim, T.; Yoo, S.; Ham, H.J.; Kang, S.Y.; Kang, S.; Cho, S.K.; Han, M.S. A hydrazone-based turn-on fluorescent probe for peroxynitrite detection and live-cell imaging. Dye. Pigment. 2019, 171, 107762.
81. Shen, Y.M.; Dai, L.C.; Zhang, Y.Y.; Li, H.T.; Chen, Y.D.; Zhang, C.X. A novel pyridinium-based fluorescent probe for ratiometric detection of peroxynitrite in mitochondria. Spectrochim. Acta A Mol. Biomol. Spectrosc. 2020, 228, 117762.
82. Parthiban, C.; Manivannan, R.; Son, Y.A. A novel near-infrared fluorescent probe for rapid detection of peroxynitrite with large stokes shift and imaging in living cells. J. Photochem. Photobiol. A 2022, 423, 113579.
83. Palanisamy, S.; Wu, P.Y.; Wu, S.C.; Chen, Y.J.; Tzou, S.C.; Wang, C.H.; Chen, C.Y.; Wang, Y.M. In vitro and in vivo imaging of peroxynitrite by a ratiometric boronate-based fluorescent probe. Biosens. Bioelectron. 2017, 91, 849–856.
84. Wang, M.M.; Wang, C.; Song, W.W.; Zhong, W.T.; Sun, T.M.; Zhu, J.L.; Wang, J. A novel borate fluorescent probe for rapid selective intracellular peroxynitrite imaging. Spectrochim. Acta A Mol. Biomol. Spectrosc. 2021, 251, 119398.
85. Kim, J.; Park, J.; Lee, H.; Choi, Y.; Kim, Y. A boronate-based fluorescent probe for the selective detection of cellular peroxynitrite. Chem. Commun. 2014, 50, 9353–9356.
86. Xia, L.L.; Tong, Y.; Li, L.S.; Cui, M.Y.; Gu, Y.Q.; Wang, P. A selective fluorescent turn-on probe for imaging peroxynitrite in living cells and drug-damaged liver tissues. Talanta 2019, 204, 431–437.
87. Jiang, G.Y.; Li, C.B.; Lai, Q.F.; Liu, X.; Chen, Q.Q.; Zhang, P.F.; Wang, J.G.; Tang, B.Z. An easily available ratiometric AIE probe for peroxynitrite in vitro and in vivo imaging. Sens. Actuators B Chem. 2021, 329, 129223.
88. Zhang, J.; Li, Y.P.; Zhao, J.J.; Guo, W. An arylboronate-based fluorescent probe for selective and sensitive detection of peroxynitrite and its applications for fluorescence imaging in living cells. Sens. Actuators B Chem. 2016, 237, 67–74.